Dynamic Analysis of the Rigid Rotor System

AKIRA AZUMA*
University of Tokyo, Tokyo, Japan

A unified dynamic analysis for the rotor motion of the rigid or nonarticulated rotor system in a hovering state is presented. The dynamic behavior of the rigid rotor as well as that of the conventional rotor is expressed in a simple linearized mathematical form by using complex variables. The available control moment and the necessary phase shift for a given cyclic pitch input are obtained in general formulas and charts. Generally, the control and damping moments of the rigid rotor system increase with the increment of the flapping stiffness, but there is a critical stiffness at which the aforementioned moments will be maximum. Optimum flapping stiffness may be given so as to avoid unfavorable coupling motion between roll and pitch. It is not always necessary to install the control gyro, because similar stabilizing effect may be obtained by using the proper blade configuration without a special gyro system. The necessary control phase advance is also given to avoid cross control of the rigid rotor system.

Nomenclature

a = lift slope
B = tip loss factor
b = number of blades
C = constant given by Eq. (22)
c = blade chord
F = shear force at flapping hinge
$f(t; K, K_\beta)$ = time reponse function given by Eq. (21)
g = gravity acceleration
h = hub location from the center of gravity
I_β = moment of inertia about flapping hinge given by Eq. (6)
I_H, I_V = horizontal and vertical inertia given by Eq. (39)
I_G = gyro moment of inertia about spin axis
$i = (-1)^{1/2}$ = imaginary
K, K_1, K_2 = constants given by Eq. (9)
K_β = nondimensional flapping stiffness given by Eq. (14)
k_β, k_ϵ = spring stiffnesses for the flapping and feathering angles
k_θ = aerodynamic and mechanical restoring stiffness for the feathering angle
$k_{\dot\theta}$ = aerodynamic and mechanical damping along the feathering axis
$k_{\beta m}$ = the k_β at which the maximum moment is obtained, given by Eq. (33)
$k_{\beta n}$ = the k_β at which no coupling motion is presented, given by Eqs. (35) or (36)
k_G = spring stiffness of control gyro
l = control rod location from the shaft
l_δ = gearing length of stick control
M_A = aerodynamic flapwise moment given by Eq. (3)
M_I = inertial flapwise moment given by Eq. (4)
M_m = mechanical flapwise moment given by Eq. (5)
M_{X_B}, M_{Y_B} = moments along the body coordinate system
$\mathbf{M}_G = \mathbf{M}_{G_a} + \mathbf{M}_{G_b}$ = complex gyro control moment given by Eq. (49)
$\mathbf{M}_B = M_{X_B} - iM_{Y_B}$ = complex body control moment given by Eq. (27)
$M_\theta = M_{\theta a} + M_{\theta b}$ = external moment along feathering axis given by Eq. (42)
m = mass of the blade element for unit width
p = rotor angular velocity along $-X$ axis
q = rotor angular velocity along Y axis
R = blade radius
R_B, R_G = geometrical quantities about feathering mechanism given by Fig. 8
r = radius of the blade element
r_c = radius of the blade cut-out
r_β = radius of the flapping hinge location
$\bar{r}$ = radius of the blade center of gravity given by Eq. (6)
S = rotor area
$T_{1/2}$ = time required to damp out to the half-amplitude
t = time
W = body weight
W_β = weight of the blade out side of the flapping hinge
X, Y, Z = rotor coordinate system; X axis is positive backward
X_B, Y_B, Z_B = body coordinate system; X_B axis is positive forward
$x = r/R$ = nondimensional radius of the blade element
$x_c = r_c/R$ = nondimensional blade cutout
$x_\beta = r_\beta/R$ = nondimensional radius of the flapping hinge location
y = nondimensional chordwise distance of the blade element
z = nondimensional height of the blade element
β = blade flapping angle measured from a plane normal to shaft
$\boldsymbol{\beta} = -\beta_{1s} + i\beta_{1c}$ = complex blade flapping angle
β_{1c}, β_{1s} = first harmonic Fourier coefficients of the flapping angle
β_0 = coning angle
γ = Lock number given by Eq. (10); also necessary phase shift to avoid cross control, given by Eq. (56)
Δ = quantity given by Eq. (53)
$\boldsymbol{\delta}_s = -\delta_\phi + i\delta_\theta$ = complex control input
δ_ϕ, δ_ϕ = control stick input
$\dot{\boldsymbol{\varepsilon}} = -p + iq = (d/dt)\,\boldsymbol{\varepsilon}$ = complex angular velocity of the rotor shaft axes
ϵ = lead caused by chordwise deformation
$\boldsymbol{\varepsilon} = -\Phi + i\Theta$ = complex body attitude
$\boldsymbol{\varepsilon}_G = -\phi_G + i\theta_G$ = complex control gyro attitude
η = lead angle of the blade elastic axis with respect to feathering axis

Received July 26, 1966; revision received November 28, 1966. [7.06]

* Associate Professor, Institute of Space and Aeronautical Science. Member AIAA.

Θ	=	pitching angle of the body
θ	=	blade feathering angle
$\boldsymbol{\theta} = -\theta_{1s} + i\theta_{1c}$	=	complex cyclic pitch
θ_0	=	collective pitch
θ_t	=	blade twist
θ_{1c}, θ_{1s}	=	first harmonic Fourier coefficients of the cyclic pitch
θ_G, ϕ_G	=	pitching and rolling angle of control gyro
λ_1, λ_2	=	characteristic roots of the equation of motion
λ_{s0}	=	constant inflow ratio
$\boldsymbol{\lambda}_s = -\lambda_{1s} + i\lambda_{1c}$	=	complex inflow ratio
$\lambda_{1c}, \lambda_{1s}$	=	first harmonic Fourier coefficients of the inflow ratio
ρ	=	air density
$\sigma = bc/\pi R$	=	solidity
Φ	=	rolling angle of the body
ϕ	=	rolling angle of the rotor
ψ	=	phase angle
Ω	=	rotor angular velocity

Superscripts

$\dot{A} = (d/dt)A$	=	time derivative of A

Subscripts

B	=	body coordinate system
G	=	gyro
C, I	=	centrifugal and inertial forces

Introduction

IT has been found that the so-called rigid or nonarticulated rotor system provides high potential, specifically in the field of stability and control of the advanced helicopter. The most attractive gain with adopting the rigid rotor concept must be the large increase in control power.

The dynamic characteristics of the rigid rotor system have been analyzed by Payne[8] and investigated practically by a few companies[1–4,7] through analytical studies, wind-tunnel tests, and flight tests. It must, however, be necessary to provide legible working charts and also to suggest an appropriate flapping or lead-lag stiffness with necessary performance for a given rotor configuration.

This paper describes a unified analysis of the dynamic rotor behavior not only for conventional or articulated rotors but also for rigid or nonarticulated rotor system by using complex variables about physical quantities of the rotor motion. The effect of the increase in flapping stiffness on the rotor dynamics as well as on control power will, therefore, be apparent from the present analysis.

Flapping Motion

In this section, a blade flapping motion of a so-called rigid rotor system operating in a hovering state will be discussed as one-degree-of-freedom motion about its flapping hinge, on which a spring is mounted so as to increase the blade flapping stiffness, as seen in Fig. 1. It is further assumed that the flapping motion will be limited by the first harmonic motion of each revolution of the rotor blade; i.e., the flapping angle β with respect to a plane being orthogonal to the rotor shaft is given by

$$\beta = \beta_0 + \beta_{1c}\cos\psi + \beta_{1s}\sin\psi \quad (1)$$

wherein ψ is the phase angle of the blade measured from one of the axes of a rotor coordinate system or from the X axis, which is normal to the shaft axis. Thus, the rotor motion is represented by the inclination of the tip path plane that responds to the control input or the body motion, but the coupled motion of the rotor and the body is not considered.

The differential equation of blade flapping motion is derived for the aforementioned assumed rotor by equating the blade aerodynamic moment M_A, inertia moment M_I, and

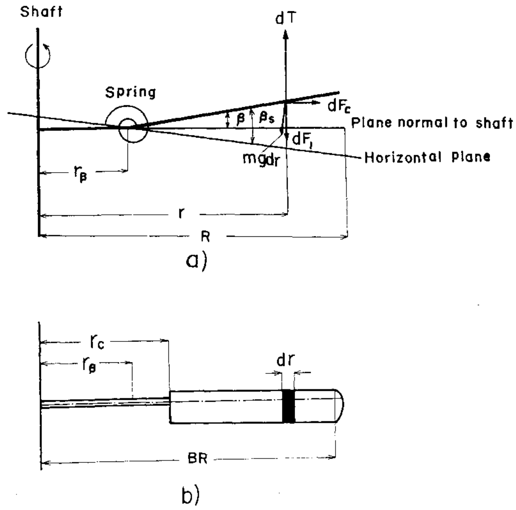

Fig. 1 Blade flapping motion.

mechanical moment M_m about the flapping hinge as follows:

$$M_A + M_I + M_m = 0 \quad (2)$$

where M_A, M_I, and M_m are, respectively, given by[5–7] (see Figs. 1 and 2)

$$M_A = \frac{1}{2}\,\rho acR^4\Omega^2\left\{\left(\frac{B^4}{4} - \frac{B^3}{3}x_\beta\right)\theta_0 + \left(\frac{B^5}{5} - \frac{B^4}{4}x_\beta\right)\times \theta_t - \left(\frac{B^3}{3} - \frac{B^2}{2}x_\beta\right)\lambda_{s0} - \left(\frac{B^4}{4} - \frac{B^3}{3}x_\beta\right)\frac{\dot\beta_0}{\Omega} + \left[\left(\frac{B^4}{4} - \frac{B^3}{3}x_\beta\right)\theta_{1c} + \left(\frac{B^4}{4} - \frac{B^3}{3}x_\beta\right)\left\{\frac{q}{\Omega} - \lambda_{1c} - \left(\frac{\dot\beta_{1c}}{\Omega} + \beta_{1s}\right)\right\}\right]\cos\psi + \left[\left(\frac{B^4}{4} - \frac{B^3}{3}x_\beta\right)\theta_{1s} + \left(\frac{B^4}{4} - \frac{B^3}{3}x_\beta\right)\left\{\frac{P}{\Omega} - \lambda_{1s} - \left(\frac{\dot\beta_{1s}}{\Omega} - \beta_{1c}\right)\right\}\right]\sin\psi\right\} \quad (3)$$

$$M_I = -I_\beta\{\ddot\beta_0 + (\ddot\beta_{1c} + 2\dot\beta_{1s}\Omega - \beta_{1s}\Omega^2 - \dot q)\cos\psi + (\ddot\beta_{1s} - 2\dot\beta_{1c}\Omega - \beta_{1c}\Omega^2 - \dot p)\sin\psi\} + \left(I_\beta + \frac{W_\beta}{g}\bar r r_\beta\right)\times \Omega^2(\beta_0 + \beta_{1c}\cos\psi + \beta_{1s}\sin\psi) + \left(I_\beta + \frac{W_\beta}{g}\bar r r_\beta\right)\times 2\Omega\,(-p\cos\psi + q\sin\psi) + \bar r W_\beta \quad (4)$$

$$M_m = -k_\beta\beta = -k_\beta(\beta_0 + \beta_{1c}\cos\psi + \beta_{1s}\sin\psi) \quad (5)$$

where

$$I_\beta = \int_{r_\beta}^{R} m(r - r_\beta)^2\,dr \qquad W_\beta\bar r = \int_{r_\beta}^{R} mg(r - r_\beta)dr \quad (6)$$

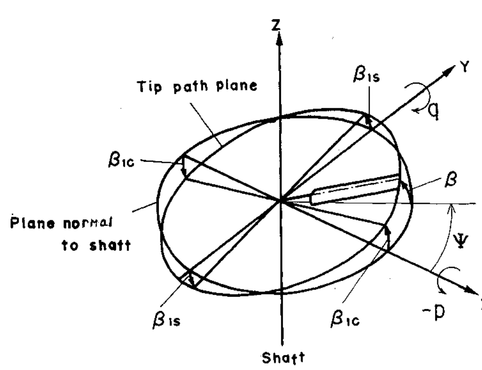

Fig. 2 Tip path plane and plane normal to shaft.

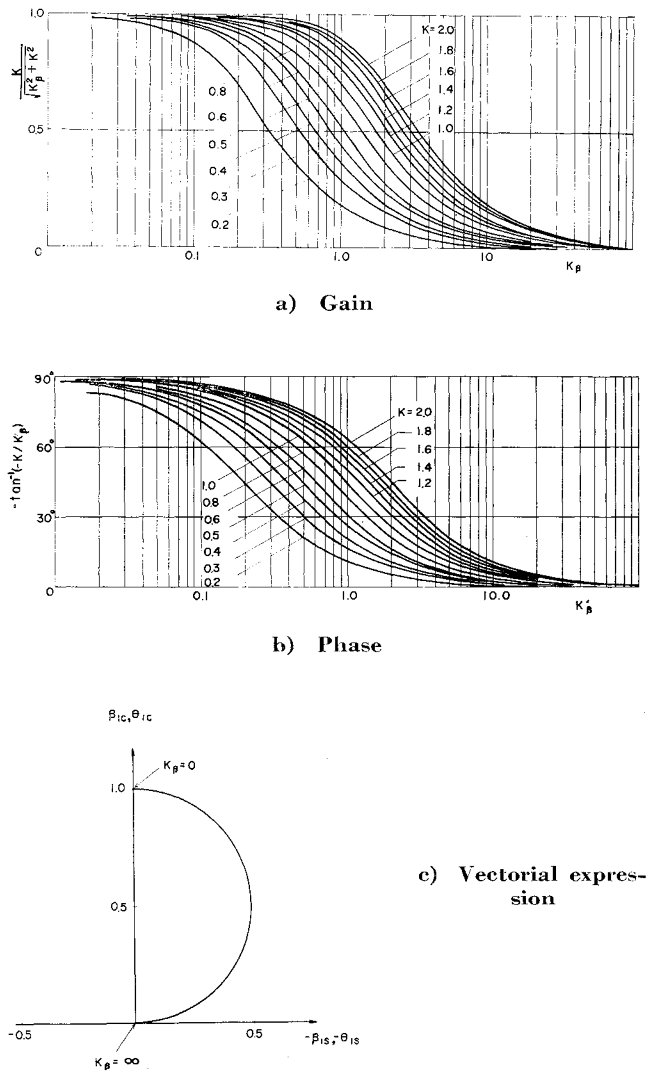

a) Gain

b) Phase

c) Vectorial expression

Fig. 3 Flapping angle in the steady terminal state.

Substituting these moments given by Eqs. (3–5) into Eq. (2), one equation for the nonsinusoidal component and the following two equations for the $\cos\psi$ and $\sin\psi$ components, which determine the rotor tilt angle with respect to shaft, are obtained, as follows:

$$\ddot{\beta}_{1c} + K\Omega\dot{\beta}_{1c} + \left\{\frac{k_\beta}{I_\beta} + \Omega^2 \frac{W_\beta}{I_\beta g}\bar{r}r_\beta\right\}\beta_{1c} + 2\Omega\dot{\beta}_{1s} + K\Omega^2\beta_{1s} = \dot{q} + 2\Omega P\left(1 + \frac{W_\beta}{I_\beta g}\bar{r}r_\beta\right) + K\Omega^2\left(\theta_{1c} + \frac{q}{\Omega} - \lambda_{1c}\right) \quad (7)$$

$$\ddot{\beta}_{1s} + K\Omega\dot{\beta}_{1s} + \left\{\frac{k_\beta}{I_\beta} + \Omega^2 \frac{W_\beta}{I_\beta g}\bar{r}r_\beta\right\}\beta_{1s} - 2\Omega\dot{\beta}_{1c} - K\Omega^2\beta_{1c} = \dot{p} - 2\Omega q\left(1 + \frac{W}{I_\beta g}\bar{r}r_\beta\right) + K\Omega^2\left(\theta_{1s} + \frac{p}{\Omega} - \lambda_{1s}\right) \quad (8)$$

where K is

$$K = \frac{\gamma}{2}\left(\frac{B^4}{4} - \frac{B^3}{3}\right)x_\beta \quad (9)$$

and γ is the Lock number, given by

$$\gamma = \rho acR^4/I_\beta \quad (10)$$

Combining Eqs. (7) and (8) with $i = (-1)^{1/2}$ as

$$\left.\begin{aligned} \boldsymbol{\beta} &= -\beta_{1s} + i\beta_{1c} \\ \boldsymbol{\theta} &= -\theta_{1s} + i\theta_{1c} \\ \boldsymbol{\lambda}_s &= -\lambda_{1s} + i\lambda_{1c} \\ \text{and} \quad \dot{\boldsymbol{\varepsilon}} &= -p + iq \end{aligned}\right\} \quad (11)$$

then a unified equation of the complex flapping angle $\boldsymbol{\beta}$ is obtained as follows:

$$\ddot{\boldsymbol{\beta}} + (K - i2)\Omega\dot{\boldsymbol{\beta}} + \left\{\left(\frac{k_\beta}{I_\beta} + \frac{W_\beta}{I_\beta g}\bar{r}r_\beta\Omega^2\right) - iK\Omega^2\right\}\boldsymbol{\beta} = \ddot{\boldsymbol{\varepsilon}} + (K - i2)\Omega\dot{\boldsymbol{\varepsilon}} + K\Omega^2(\boldsymbol{\theta} - \boldsymbol{\lambda}_s) \quad (12)$$

Steady Terminal State

For steady flight, i.e., $p = q = 0$, the terminal state of the flapping motion is given by Eq. (12) as

$$\boldsymbol{\beta} = \frac{Ke^{-i\tan^{-1}(-K/K_\beta)}}{(K_\beta^2 + K^2)^{1/2}} \cdot (\boldsymbol{\theta} - \boldsymbol{\lambda}_s) \quad (13)$$

wherein

$$K_\beta = \frac{k_\beta}{I_\beta}\frac{1}{\Omega^2} + \frac{W_\beta}{I_\beta g}\bar{r}r_\beta \quad (14)$$

The preceding results correspond to those obtained in Ref. 8.

For the conventional or free-flapping rotor, the following approximation may be established:

$$\left.\begin{aligned} (K_\beta^2 + K^2)^{1/2} &= K \\ e^{-i\tan^{-1}(-K/K_\beta)} &= e^{-i(-\pi/2)} = i \end{aligned}\right\} \quad (15)$$

Also, for the special case in which $\lambda_{1c} = \lambda_{1s} = 0$ (constant inflow distribution), Eq. (13) will give the following simple relation:

$$\boldsymbol{\beta} = i\boldsymbol{\theta} \quad \text{or} \quad \boldsymbol{\theta} = -i\boldsymbol{\beta} \quad (16)$$

For spring-constrained or rigid rotors, it will be appreciated that the complex flapping angle $\boldsymbol{\beta}$ will change in both magnitude and phase corresponding to the coefficient $[K/(K_\beta^2 + K^2)^{1/2}]e^{-i\tan(-K/K_\beta)}$ of Eq. (13).

K_β, which is an equivalent spring stiffness given in Eq. (14), will change from a small value to infinity as the spring stiffness increases, whereas K is the damping term given by Eq. (9) and is affected mainly by the Lock number. The Lock number will usually fall in the range of $\gamma = 3$–12, and hence it may be assumed that K falls within a range from zero to two. In many cases, the aerodynamic damping about the flapping motion is substantially large, so that the mechanical damping as well as blade-pitch feedback due to flapping may not be necessary.

For the estimation of the $[K/(K_\beta^2 + K^2)^{1/2}]e^{-i\tan^{-1}(-K/K_\beta)}$, Figs. 3a and 3b show the graphical representations of $K/(K_\beta^2 + K^2)^{1/2}$ and $-\tan^{-1}{}_{(-K/K_\beta)}$, respectively, for various values of K_β and K.

From these figures it will be seen that as the spring stiffness or K_β increases, the phase will decrease from 90° to 0°, and the gain will decrease from 1 to 0; also, predominant change will occur within $K_\beta = 0.1$–10 or, more limitedly speaking, around $K_\beta = 1.0$. It may, therefore, be appreciated that in a complex plane the vector of the flapping angle will trace on a semicircle for any K, as shown in Fig. 3c; and if only one-direction cyclic pitch $-\theta_{1s}$ is introduced, the tilt angle of the tip path plane will be reduced as spring stiffness increases and the tilt direction will change from forward to rightward.

Transient Rotor Behavior

In order to trace the transient motion of the tip path plane, the characteristic roots of Eq. (12) must first be found, such as

$$\begin{matrix}\lambda_1 \\ \lambda_2\end{matrix} = -\tfrac{1}{2}K\Omega + i\Omega\,\{1 \pm [1 + K_\beta - (K/2)^2]^{1/2}\} \quad (17)$$

As previously mentioned, the aerodynamic damping $K\Omega$ is generally large enough to damp out the rotor motion within a reasonable time compared with the helicopter body motion. It is usually realized that in Eq. (17)

$$1 + K_\beta - (K/2)^2 \geq 0 \quad (18)$$

Within the range of $K = 0.5$–2.0 with $\Omega = 30\ \text{sec}^{-1}$, the time required to damp out the half-amplitude $T_{1/2}$ is about $\frac{1}{10}$ sec–$\frac{1}{50}$ sec. It will, therefore, be appreciated that Hohenemser's assumption, under which the blade dynamics can be treated as a sequence of steady-state conditions, may still be valid even for the rigid rotor.

Now, let us consider the flapping response for the body motion. The flapping equation due to the body motion will be given by

$$\ddot{\boldsymbol{\beta}} + (K - i2)\Omega\dot{\boldsymbol{\beta}} + (K_\beta - iK)\Omega^2\boldsymbol{\beta} = \ddot{\boldsymbol{\varepsilon}} + (K - i2)\Omega\dot{\boldsymbol{\varepsilon}} \quad (19)$$

For the step input of $\dot{\boldsymbol{\varepsilon}}$, $\boldsymbol{\beta}\,(t)$ will be given as

$$\boldsymbol{\beta} = \frac{\dot{\boldsymbol{\varepsilon}}}{\Omega}\left(\frac{K^2 + 4}{K^2 + K_\beta^2}\right)^{1/2} e^{i\tan^{-1}[(K^2 - 2K_\beta)/K(2+K_\beta)]} \times f(t; K, K_\beta) + \frac{\dot{\boldsymbol{\varepsilon}}}{2C\Omega}\, e^{[-(1/2)k+i]\Omega t - i(\pi/2)} \times \{e^{i\Omega Ct} - e^{-i\Omega Ct}\} \quad (20)$$

wherein

$$f(t; K, K_\beta) = 1 + e^{[-(1/2)K+i]\Omega t}\left\{\frac{(2 + K_\beta - 2C)^{1/2}}{2C} \times e^{i[\Omega Ct + \tan^{-1}(K/2)/(1-C)]} - \frac{(2 + K_\beta + 2C)^{1/2}}{2C} \times e^{i[-\Omega Ct + \tan^{-1}\{(K/2)/(1+C)\}]}\right\} \quad (21)$$

and

$$C = [1 - (K/2)^2 + K_\beta]^{1/2} \quad (22)$$

Then the terminal conditions are given by

$$\text{at } t = 0 \qquad \boldsymbol{\beta} = 0$$

$$\text{at } t = \infty \qquad \boldsymbol{\beta} = \frac{\dot{\boldsymbol{\varepsilon}}}{\Omega}\left(\frac{K^2 + 4}{K^2 + K_\beta^2}\right)^{1/2} \times e^{i\tan^{-1}[(K^2 - 2K\beta)/K(2+K_\beta)]} \quad (23)$$

It must be noted that even in the case of the free-flapping rotor there is some phase shift between $\boldsymbol{\beta}$ and $\dot{\boldsymbol{\varepsilon}}$.

The response for the cyclic pitch input is given from the following equation:

$$\ddot{\boldsymbol{\beta}} + (K - i2)\Omega\dot{\boldsymbol{\beta}} + (K_\beta - iK)\Omega^2\boldsymbol{\beta} = \Omega^2 K\boldsymbol{\theta} \quad (24)$$

For the step input of $\boldsymbol{\theta}$, the time response is given by

$$\boldsymbol{\beta}(t) = \frac{K\boldsymbol{\theta}}{(K_\beta^2 + K^2)^{1/2}}\, e^{-i\tan^{-1}(-K/K_\beta)} \cdot f(t; K, K_\beta) \quad (25)$$

The terminal state of the preceding equation has already been discussed in Eq. (13).

The function $f(t; K, K_\beta)$ will characterize the time response of the rotor system, so that the remaining part of this section will be devoted to the discussion of this time-response function of the rotor.

As examples, let the following parameters of the $f(t; K, K_\beta)$ be selected:

$$K = 1 \qquad K_\beta = 0, 1, 10$$

and

$$\Omega = 30\ \text{rad/sec} \quad (26)$$

Figures 4a-c show the time-response curves of the $f(t; K, K_\beta)$ for the unit step input. In these figures, each of two fine curves shows the respective two terms of Eq. (21), and their origins are shifted from -1 to 0. Each thick line in the figures shows the whole response of $f(t; K, K_\beta)$ corresponding to $K_\beta = 0$, 1, and 10, respectively.

It will be seen from the figures that as K_β increases, the amount of coiling about a terminal point and the number of modes or cusps become large but the elapsed time remains constant. If K_β increases, the twisting around the terminal point is also changed from a counter-clockwise to a clockwise direction or from a similar direction to rotor rotation, because of the sign change of $1 - C$. Although the rotor tilts very quickly for large K_β, the vibration of the rotor mast must be more severe than the vibration of the free-flapping rotor.

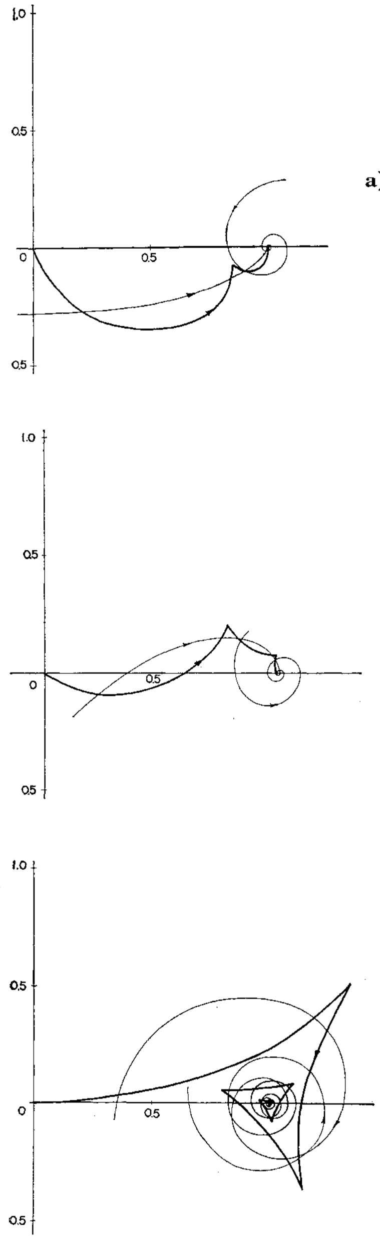

a) $K_\beta = 0 (K = 1, \Omega = 30\ \text{sec}^{-1})$

b) $K_\beta = 1.0 (K = 1, \Omega = 30\ \text{sec}^{-1})$

c) $K_\beta = 10 (K = 1, \Omega = 30\ \text{sec}^{-1})$

Fig. 4 Step response of the flapping angle.

Hub Moments

In this section the moment acting on the hub of a single rotor will be analyzed. The complex body moment in a hovering state will approximately be given by

$$\mathbf{M}_B = M_{XB} - iM_{YB} \tag{27}$$

$$= \frac{\sigma}{2}\rho S(R\Omega)^2 r_\beta \frac{B^3}{6}(\boldsymbol{\theta} + i\boldsymbol{\beta} - \boldsymbol{\lambda}_s) + \frac{b}{2}k_\beta\boldsymbol{\beta} + \frac{b}{2}(ik_\theta + k_{\dot\theta}\,\Omega)\boldsymbol{\theta} + \frac{b}{2}\frac{W_\beta}{g}r_\beta(\bar r + r_\beta)\boldsymbol{\beta}\Omega^2 + i2\Omega\frac{b}{2}\frac{W_\beta}{g}r_\beta(\bar r + r_\beta)\dot{\boldsymbol{\varepsilon}} + Wh\boldsymbol{\beta}$$

Since the relation (16) has been established, in the free-flapping rotor the first and second terms of the aerodynamic components in the foregoing equation may be canceled out. Even in the case of the rigid rotor, either the aerodynamic terms

$$\frac{\sigma}{2}\rho S(R\Omega)^2 r_\beta \frac{B^3}{6}(\boldsymbol{\theta} + i\boldsymbol{\beta} - \lambda s)$$

or the feathering stiffness

$$\frac{b}{2}(ik_\theta + k_{\dot\theta}\Omega)\boldsymbol{\theta}$$

are so small compared to the remaining terms that the control moment of Eq. (27) will be approximated as

$$\mathbf{M}_B = \left\{\frac{b}{2}k_\beta + \frac{b}{2}\frac{W_\beta}{g}r_\beta(\bar r + r_\beta)\Omega^2 + Wh\right\}\boldsymbol{\beta} + i2\Omega\frac{b}{2}\frac{W_\beta}{g}r_\beta(\bar r + \bar r_\beta)\dot{\boldsymbol{\varepsilon}} \tag{28}$$

Under the present assumption, the flapping angle $\boldsymbol{\beta}$ will be rewritten from Eqs. (13) and (23) as

$$\boldsymbol{\beta} = \frac{K}{(K_\beta^2 + K^2)^{1/2}}e^{i\tan^{-1}[(-K/K_\beta)]}(\boldsymbol{\theta} - \boldsymbol{\lambda}) + \frac{\dot{\boldsymbol{\varepsilon}}}{\Omega}\left(\frac{K^2+4}{K^2+K_\beta^2}\right)^{1/2}e^{i\tan^{-1}[(K^2-2K_\beta)/K(2+K_\beta)]} \tag{29}$$

Thus, the control moment of a helicopter due to cyclic pitch is given by

$$\frac{\mathbf{M}_B}{\boldsymbol{\theta}} = \left[\left(\frac{b}{2}k_\beta + \frac{b}{2}\frac{W_\beta}{g}r_\beta(\bar r + r_\beta)\Omega^2 + Wh\right)\times K/(K_\beta^2 + K^2)^{1/2}\right]e^{-i\tan^{-1}(-K/K_\beta)} \tag{30}$$

In the case of the free-flapping rotor or $k_\beta = 0$ and $K_\beta \ll K$, the aforementioned moment will be approximated by

$$\frac{\mathbf{M}_B}{\boldsymbol{\theta}} = i\left\{\frac{b}{2}\frac{W_\beta}{g}r_\beta(\bar r + r_\beta)\Omega^2 + Wh\right\} \tag{31}$$

This is the well-known result for the control moment of the conventional rotor system.

In the rigid rotor system, however, the change of the absolute control moment because of the flapping stiffness variation is given by

$$\frac{\partial}{\partial k_\beta}\left|\frac{\mathbf{M}_B}{\boldsymbol{\theta}}\right| = \frac{K}{(K^2 + K_\beta^2)^{3/2}}\left[\frac{b}{2}K^2 - K_\beta\left\{\frac{b}{2}\frac{W_\beta}{I_\beta g}r_\beta(\bar r + r_\beta) + \frac{Wh}{I_\beta\Omega^2}\right\}\right] \tag{32}$$

Thus the maximum control moment will be given at

$$K_\beta = \frac{b}{2}K^2\Big/\left\{\frac{b}{2}\frac{W_\beta}{I_\beta g}r_\beta(\bar r + r_\beta) + \frac{Wh}{I_\beta\Omega^2}\right\} \equiv K_{\beta m} \tag{33}$$

The damping moment due to the body turning rate $\dot{\boldsymbol{\varepsilon}}$ is given from Eqs. (28) and (29) as

$$\frac{\mathbf{M}_\beta}{\dot{\boldsymbol{\varepsilon}}} = \frac{1}{\Omega}\left(\frac{K^2+4}{K^2+K_\beta^2}\right)^{1/2}e^{i\tan^{-1}[(K^2-2K_\beta)/K(2+K_\beta)]}\times\left\{\frac{b}{2}k_\beta + \frac{b}{2}\frac{W}{g}r_\beta(\bar r + r_\beta)\Omega^2 + Wh\right\} + i2\Omega\frac{b}{2}\frac{W_\beta}{g}r_\beta(\bar r + r_\beta) \tag{34}$$

In the aforementioned damping moment it may be important to reduce the phase difference between the damping moment and turning velocity. This will be attained by keeping the following relation:

$$K_\beta^2\left\{\frac{I_\beta g}{W_\beta r_\beta(\bar r + r_\beta)} - 1\right\} + 2K_\beta\left\{\frac{Wh}{b(W_\beta/g)r_\beta(\bar r + r_\beta)\Omega^2} - \frac{(K^2/4)I_\beta g}{W_\beta r_\beta(\bar r + r_\beta)} - \frac{1}{2}\frac{r_\beta}{\bar r + r_\beta}\right\} - K^2\left\{1 + \frac{Wh}{b(W_\beta/g)\,r_\beta(\bar r + r_\beta)\Omega^2} + \frac{1}{2}\frac{r_\beta}{\bar r + r_\beta}\right\} = 0 \tag{35}$$

In the foregoing equation it will be assumed that $r_\beta \ll \bar r$ and the term $I_\beta g/W_\beta r_\beta(\bar r + r_\beta)$ will be predominant for the usual rotor configuration, or the second term of Eq. (34) may be neglected; therefore, the flapping stiffness causing no coupling motion, $K_{\beta n}$, may be given by

$$K_{\beta n} \doteqdot K^2/2 \tag{36}$$

If a more precise value for $K_{\beta n}$ is needed, a positive solution of Eq. (35) will have to be obtained, which is a little bigger than the $K_{\beta n}$ of Eq. (36).

It may be interesting to say that in conventional rotor configurations the relation $K_{\beta m} \gg K_{\beta n}$ is established. Therefore it may be desirable to select the flapping stiffness as $K_\beta = K_{\beta n}$ as long as sufficient control moment is still obtained for such a configuration. Hence the damping moment will then be given by

$$\frac{\mathbf{M}_B}{\dot{\boldsymbol{\varepsilon}}} = \frac{1}{\Omega}\frac{K(K_{\beta n} + 2)}{K_{\beta n}^2 + K^2}\left[\frac{b}{2}I_\beta\Omega^2\times\left\{K_{\beta n} + \frac{W_\beta}{I_\beta g}r_\beta(\bar r + r_\beta)\right\} + Wh\right] \tag{37}$$

If the aforementioned assumption [that the second term of Eq. (34) is neglected as a small quantity] is still effective, the maximum value of $|\mathbf{M}_B/\boldsymbol{\varepsilon}|$ will also be given at $K_\beta = K_{\beta m}$.

Feathering Motion

A study of the free-feathering blade motion will be considered in this section for a balanced rotor system that is controlled either through a control gyro or directly from the swash plate sustained with a spring system. The spring is installed either on the first control rod, located between the pilot's stick and the swash plate, or on the second control rod, located between the swash plate and the control gyro, to balance the feathering motion of the rotor blade (see Fig. 5).

By referring to Fig. 6, the feathering motion will be obtained as[1]

$$(I_H + I_V)\ddot\theta + k_{\dot\theta}\dot\theta + \{k_\theta + (I_H - I_V)\Omega^2\}\theta = M_\theta \tag{38}$$

where M_θ is the external moment along the feathering axis, k_θ and $k_{\dot\theta}$ are restoring and damping moments, respectively, caused by the aerodynamic force and, if necessary, mechanical

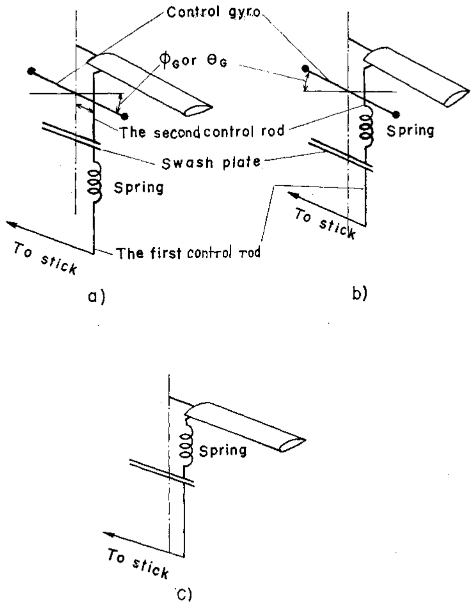

Fig. 5 Control mechanism.

arrangement installed on the feathering axis, and I_H and I_V are moments of inertia given by

$$\left.\begin{aligned} I_H &= \textstyle\iiint c^2y^2dm \qquad \text{(horizontal inertia)} \\ I_V &= \textstyle\iiint c^2z^2dm \qquad \text{(vertical inertia)} \end{aligned}\right\} \tag{39}$$

The external moment M_θ consists of two parts, one of which is the moment due to the blade deformation and the other the forced moment given from either the control gyro or the swash plate itself.

As can be seen from Fig. 7, the moment given from the blade deformation, $M_{\theta a}$, is

$$M_{\theta a} = k_\beta \beta\eta + \beta\epsilon(k_\epsilon - k_\beta) \tag{40}$$

and if the elastically matched rotor is used, the preceding equation will be

$$M_{\theta a} = k_\beta\beta\eta \tag{41}$$

Usually, η is so small a quantity that the $M_{\theta a}$ can be neglected.

The remaining external moment $M_{\theta b}$ is then expressed as

$$\begin{aligned} M_{\theta b} &= M_\theta - M_{\theta a} \\ &= (I_H + I_V)\ddot{\theta} + k_{\dot\theta}\dot{\theta} + \{k_\theta + (I_H - I_V)\Omega^2\}\,\theta \end{aligned} \tag{42}$$

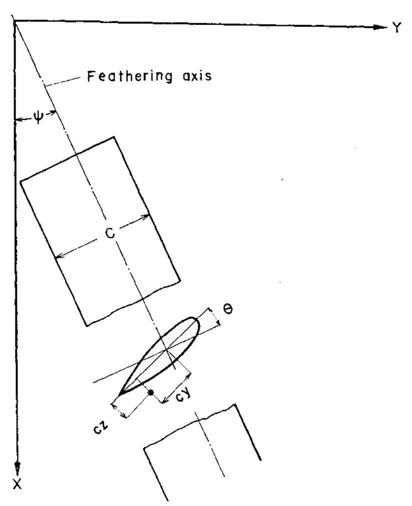

Fig. 6 Feathering motion of the blade element.

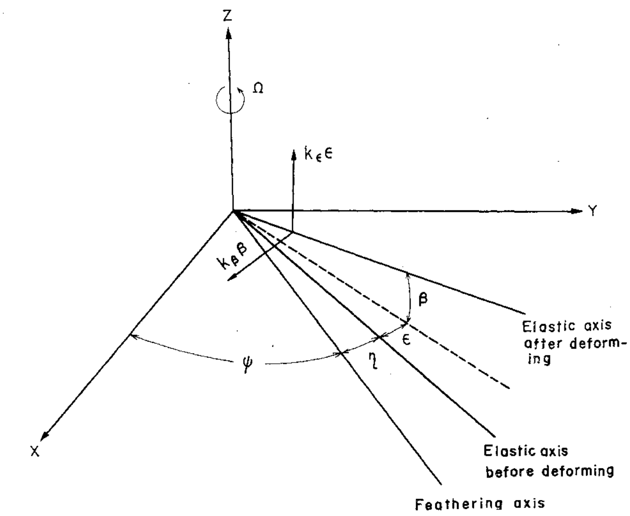

Fig. 7 Moment caused by blade deformation.

Since the $M_{\theta b}$ is the external moment for the blade feathering motion, the $-M_{\theta b}$ must be an external moment for the control gyro motion. Thus the resolution of rolling and pitching moments applied to the control gyro by a single blade, as shown in Fig. 8, yields

$$\begin{aligned} -M_{XG_1} &= (R_G/R_B)M_{\theta b}\sin(\psi + \gamma) \\ M_{YG_1} &= (R_G/R_B)M_{\theta b}\cos(\psi + \gamma) \end{aligned} \tag{43}$$

By using Eq. (42) and the geometrical relation

$$\theta = -(R_G/R_B)\{(\theta_G - \Theta)\cos(\psi + \gamma) + (\phi_G - \Phi)\sin(\psi + \gamma)\} + \theta_0 \tag{44}$$

the resultant moment for whole blade will be given by

$$\begin{aligned} \mathbf{M}_{Gb} &= M_{XGb} + iM_{YGb} \\ &= (b/2)(R_G/R_B)^2[(I_H + I_V)\{-(\ddot{\boldsymbol{\varepsilon}}_G - \ddot{\boldsymbol{\varepsilon}}) + i2\Omega(\dot{\boldsymbol{\varepsilon}}_G - \dot{\boldsymbol{\varepsilon}})\} + k_{\dot\theta}\{-(\dot{\boldsymbol{\varepsilon}}_G - \dot{\boldsymbol{\varepsilon}}) + i\Omega(\boldsymbol{\varepsilon}_G - \boldsymbol{\varepsilon})\} - \\ &\qquad (k_\theta - 2I_V\Omega^2)(\boldsymbol{\varepsilon}_G - \boldsymbol{\varepsilon})] \end{aligned} \tag{45}$$

where k_θ and $k_{\dot\theta}$ are assumed to be independent on the blade position and

$$\boldsymbol{\varepsilon}_G = -\phi_G + i\theta_G \tag{46}$$

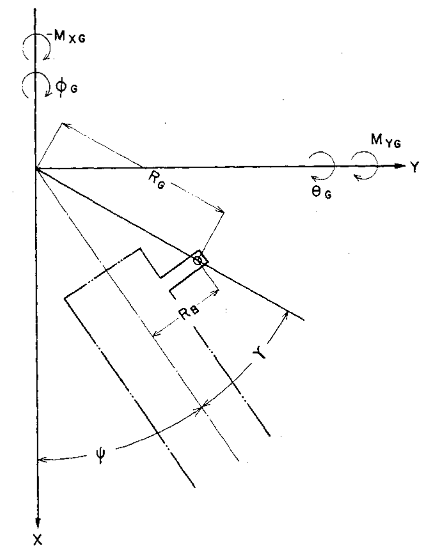

Fig. 8 Geometry of the feathering mechanism.

The gyro control moment $\mathbf{M}_{Ga}$ will be given by a control stick deflection through a spring, as shown in Fig. 5

$$\begin{aligned}\mathbf{M}_{Ga} &= M_{XGa} + iM_{YGa} \\ &= k_G\{l_\delta\boldsymbol{\delta}_s - l(\boldsymbol{\varepsilon}_G - \boldsymbol{\varepsilon})\}\end{aligned} \tag{47}$$

where

$$\boldsymbol{\delta}_s = -\delta_\phi + i\delta_\theta \tag{48}$$

Since the equation of gyro motion is given by

$$\mathbf{M}_G = \mathbf{M}_{Ga} + \mathbf{M}_{Gb} = (I_G/2)(\ddot{\boldsymbol{\varepsilon}}_G - i2\Omega\,\dot{}_G) \tag{49†}$$

the following equation will be obtained:

$$\begin{aligned}&\ddot{\boldsymbol{\varepsilon}}_G\{I_G + b(R_G/R_B)^2(I_H + I_V)\} + \\ &\quad\dot{\boldsymbol{\varepsilon}}_G[b(R_G/R_B)^2k_{\dot\theta} - i2\Omega\{I_G + b(R_G/R_B)^2 \times \\ &(I_H + I_V)\}] + \boldsymbol{\varepsilon}_G[\{2k_Gl + b(R_G/R_B)^2(k_\theta - \\ &2I_V\Omega^2)\} - i\Omega b(R_G/R_B)^2k_{\dot\theta}] = \{2k_Gl_\delta\}\boldsymbol{\delta}_s - \\ &\quad\{b(R_G/R_B)k_\beta\eta e^{i\gamma}\}\boldsymbol{\beta} + b(R_G/R_B)^2\cdot[(I_H + \\ &I_V)\ddot{\boldsymbol{\varepsilon}} + \{k_{\dot\theta} - i2\Omega(I_H + I_V)\}\dot{\boldsymbol{\varepsilon}} + \{(k_\theta - \\ &\qquad 2I_V\Omega^2) - i\Omega k_{\dot\theta}\}\boldsymbol{\varepsilon}] + 2k_Gl\boldsymbol{\varepsilon}\end{aligned} \tag{50}$$

The relation between complex cyclic pitch $\boldsymbol{\theta}$ and the gyro tilt angle $\boldsymbol{\varepsilon}_G$ will be given by the relation (44) as:

$$\boldsymbol{\theta} = -(R_G/R_B)e^{-i\gamma}\cdot(\boldsymbol{\varepsilon}_G - \boldsymbol{\varepsilon}) \tag{51}$$

Consequently, Eq. (50) may also be considered as the cyclic feathering equation.

From Eqs. (50) and (51) it will be appreciated that the high-frequency-body motion will be attenuated by the large I_G so that the control gyro is necessary to compensate the gust reaction, but is not essential, as shown in Fig. 5c, for the stability and control of the rotor system itself if R_G/R_B and $I_H + I_V$ are properly selected.

Now, by neglecting the flapping term in the right-hand side of Eq. (50) and assuming the proper inertia for the blade feathering motion, i.e.,

$$b(R_G/R_B)^2k_{\dot\theta}/2\Omega\{I_G + b(R_G/R_B)^2(I_H + I_V)\} \doteqdot 0.1$$

the characteristic roots of Eq. (50) will be approximated by

$$\begin{matrix}\lambda_1 \\ \lambda_2\end{matrix} \doteqdot -\frac{\dfrac{b}{2}\left(\dfrac{R_G}{R_B}\right)^2 k_{\dot\theta}}{I_G + b\left(\dfrac{R_G}{R_B}\right)^2(I_H + I_V)} + i\Omega\,\{1 \pm (1 + \Delta)^{1/2}\} \tag{52}$$

wherein Δ is given by

$$\Delta = \frac{2k_Gl + b(R_G/R_B)^2(k_\theta - 2I_V\Omega^2)}{\{I_G + b(R_G/R_B)^2(I_H + I_V)\}\Omega^2} \tag{53}$$

and may be a very small quantity ($\Delta \ll 1$). Hence, the higher-frequency term of Eq. (50) can be neglected and the gyro attitude for the control input will be approximated by the first-order complex equation as follows‡:

$$\begin{aligned}\dot{\boldsymbol{\varepsilon}}_G + \left\{\frac{(b/2)(R_G/R_B)^2k_{\dot\theta}}{I_G + b(R_G/R_B)^2(I_H + I_V)} + i\left(\frac{\Delta}{2}\right)\Omega\right\}\boldsymbol{\varepsilon}_G = \\ i(2k_Gl_\delta)\boldsymbol{\delta}_s/2\Omega\{I_G + b(R_G/R_B)^2(I_H + I_V)\}\end{aligned} \tag{54}$$

† It is assumed here that the moment of inertia of the swash plate is negligibly small.

‡ A similar approximation will be applicable to Eq. (12) when $K_\beta \doteqdot (K/2)^2$, as seen in Eq. (17).

wherein the phase shift i on the top of the right-hand side of the equation is an approximation of

$$\exp(i\tan^{-1}[2\Omega\{I_G + b(R_G/R_B)^2(I_H + I_V)\}/b(R_G/R_B)^2k_{\dot\theta}])$$

The transient motion of the foregoing system will quickly and directly damp out because the damping coefficient has the order of 0.1Ω, and also the frequency $(\Delta/2)\Omega$ is very small. Thus the complex pitch angle is soon attained, as

$$\boldsymbol{\theta} = \left(\frac{-(R_G/R_B)e^{-i\tan^{-1}[-b\Omega(R_G/R_B)^2k_{\dot\theta}/\{2k_Gl + b(R_G/R_B)^2(k_\theta - 2I_V\Omega^2)\}]}}{[\{2k_Gl + b(R_G/R_B)^2(k_\theta - 2I_V\Omega^2)\}^2 + b^2\Omega^2(R_G/R_B)^4k_{\dot\theta}^2]^{1/2}}\right)2k_Gl_\delta e^{-i\gamma}\cdot\boldsymbol{\delta}_s \tag{55}$$

Substituting the foregoing relation into Eq. (30), it will be found that to avoid the cross control, the phase shift γ should be

$$\begin{aligned}\gamma = -\tan^{-1}(-K/K_\beta) - \tan^{-1}[-b\Omega(R_G/R_B)^2k_{\dot\theta}/\{2k_Gl + \\ b(R_G/R_B)^2(k_\theta - 2I_V\Omega^2)\}]\end{aligned} \tag{56}$$

In actual application the foregoing phase shift will be obtained by an additional means that will make up the phase shift given by the mechanism of Fig. 8.

Conclusion

The unified mathematical treatment of the rotor dynamics for either rigid or conventional rotor systems has been presented. The dynamic rotor behavior in the first harmonics has been shown for various flapping stiffnesses. The available control moment and the necessary phase shift for a given cyclic pitch input have been obtained in the charts (Figs. 3a–c) and shown as a semicircle. It has been noted that an optimum flapping stiffness may be given for a given rotor configuration, so as to avoid unfavorable coupling motion between roll and pitch. By proper selection of the damping or the moment of inertia about the feathering motion, i.e., $k_{\dot\theta}/2\Omega(I_H + I_V) = 0(10^{-1})$, the control gyro may be omitted if the gust reaction is not essential. The control phase advance necessary to avoid cross control of the rigid rotor system has also been given by Eq. (56).

References

[1] Yeates, J. E. and McHugh, J. C., "Investigation of elastic coupling phenomena of high speed rigid rotor systems," U. S. Army, Transport Research and Engineering Command, TR 63-75 (1964).

[2] Heppe, R. R., "The single-rotor helicopter with rigidly-mounted blades," J. Roy. Aeron. Soc. **67**, 651–663 (October 1963).

[3] Turner, A. W. et al., "Exploration of high-speed flight with the XH-51A rigid rotor helicopter," Lockheed-California Co. Report, L. R. 18374; also U. S. Army, Transport Research and Engineering Command, TR 65-25 (1965).

[4] McCloud, J. L., III and Biggers, J. C., "Full-scale wind-tunnel test of a nonarticulated helicopter rotor," NASA TN D-2392 (1964).

[5] Marinescu, A., "Über die Dynamische Stabilität der Hubschrauber mit Elastisch Angeschlossenen Rotorlättern," Z. Flugwissenschaften **13**, 7, 255–263 (1965).

[6] Gessow, A. and Crim, A. D., "A method for studying the transient blade-flapping behavior of lifting rotor at extreme operating conditions," NACA TN 3366 (1955).

[7] Cresap, W. L., "Rigid rotor development and flight tests," IAS Paper 62–17 (1962).

[8] Payne, P. R., *Helicopter Dynamics and Aerodynamics* (Sir Isaac Pitman & Sons Ltd., London, 1959), 1st ed., Chap. 4, pp. 149–180.